Determination of migration efficiency of amino alcohol based migrating corrosion inhibitor through concrete

R. Vedalakshmi*[1], K. Rajagopal[2] and N. Palaniswamy[1]

The migration efficiency of an amino alcohol based migrating corrosion inhibitor (MCI) through hardened concrete of two different strengths (20 and 30 MPa) with two different thicknesses (25 and 40 mm) has been studied using diffusion test cell arrangement. The corrosion current I_{corr} was measured using Tafel extrapolation technique. There is a 20 times reduction in I_{corr} of steel in presence of MCI compared to that of bare steel. The migration efficiency decreases with an increase in thickness as well as strength of concrete. The density of concrete influences the diffusion rate of MCI. The diffusion rate is two times higher in 20 MPa concrete than that of 30 MPa concrete. The studies have indicated that the passive layer formed on the rebar surface is not stable in presence of 1% of chloride in 20 MPa concrete. Because of higher chloride threshold level the MCI has performed better in 30 MPa concrete. The results conclude that if higher protection efficiency is needed where structure is exposed to high chloride environments, it is more appropriate that the MCI shall be added at the rate of $2 \cdot 45$ kg m^{-3} along with concrete/ repair mortar than applied on the concrete surface.

Keywords: Migrating inhibitor, Migration efficiency, Inhibition efficiency, Corrosion current, Passive layer, Tafel extrapolation technique, EIS technique

Introduction

Durability of reinforced concrete structures in marine environment is drastically reduced by reinforcement corrosion. Additions of inhibitors to concrete, use of coated rebars, surface coatings on concrete surface, electrochemical protection etc. are the most commonly adopted preventive measures. Use of corrosion inhibitors is more attractive from the point of view of economics and ease of application. Normally inhibitors are either added with the fresh concrete mixtures or externally applied on hardened concrete surface. The former can be adopted only in new concrete structures whereas the latter (migrating/penetrating inhibitor) can be applied during rehabilitation of concrete structures since they can diffuse into the hardened concrete. In concrete, both organic and inorganic inhibitors have been used. Inorganic inhibitors such as nitrite and sodium monofluoro phosphate modify the oxide film on the steel rebar and make it more protective.[1–4] The chloride ion threshold value is increased which prevents initiation of corrosion.[5] Organic inhibitors are based on mixtures of alkanolamines and amines or amino carboxylate.[6] They adsorbed on to the metal surface,

creating a monomolecular barrier which reduces both anodic and cathodic reactions. They are volatile and are able to penetrate through the capillary structure of concrete by liquid diffusion through capillary suction and also through hairline cracks and microcracks present in the concrete.[7,8] Migrating inhibitors are used in matured reinforced concrete structures that are showing signs of reinforcement corrosion or need additional protection to inhibit likely corrosion in future. They are applied on to the surface as liquids or as solid 'plugs' inserted in drilled holes which migrate through the concrete and reach the reinforcement.[9,10] Efficiency of migrating inhibitor has been studied in mortar/concrete and in simulated pore solutions.[11–15] The optimum concentration arrived was 1%. The diffusion of inhibitor through the concrete was identified using amino sensitive electrode and by measuring radioactivity levels.[16,17] With regard to diffusion of migrating corrosion inhibitor (MCI) through mortar/ concrete, it has been reported that only the diffusion of the volatile phase is measured and the diffusion of the non-volatile (carboxylate compound) through the concrete is not proved and assumed to be slow.[18] Diffusion studies have also been carried out by monitoring the MCI through the concrete by sectioning the concrete and determining the total nitrogen content in each section by secondary neutral mass spectrometry (SNMS).[19] Portanguen et al.[20] detected sodium monofluorophosphate in concrete using ion exchange chromatography and fluoride ion selective electrode. The

[1]Corrosion Protection Division, Central Electrochemical Research Institute, Karaikudi 630 006, TamilNadu, India
[2]Department of Civil Engineering, A. C. College of Engineering and Technology, Karaikudi 630 007, TamilNadu, India

*Corresponding author, email corrveda@yahoo.co.in

migration of inhibitor through the mortar was studied by electrochemical impedance spectroscopic technique by varying the thickness of the mortar.[21] Morris et al.[22] proved the migration of inhibitor through the concrete by observing the decrease in I_{corr} and increase in concrete resistance with time.

The aim of this work is to evaluate the migration efficiency of amino-alcohol based MCI (Ferrogard 903) through concrete by Tafel extrapolation technique and to discuss the mechanism of protection.

Experimental

Materials and mix proportions

Concrete mix proportions having design compressive strengths of 20 and 30 MPa at 28 days curing time were used for casting the concrete specimens. The details are given in Table 1. Ordinary Portland cement (43 grade – equivalent to ASTM type – I cement) conforming to bureau of Indian standard (BIS): 8112 (Ref. 23) (ASTM C150 specification for Portland cement) was used. Chemical composition of cement is given in Table 2. Well graded river sand and good quality crushed blue granite stone were used as fine and coarse aggregate respectively. The different size fractions of coarse aggregate (20 and 12·5 mm down graded) were taken and recombined to a specified grading as shown in Table 3. Cold twisted high yield strength deformed bar of 10 mm in diameter (Fe 415) grade conforming to IS: 1786 (Ref. 24) (ASTM A615/A615 M: specification for plain billet steel bars for concrete reinforcement) was used and its chemical composition % was C–0·17; Mn–0·66; Si–0·11; S–0·017; P–0·301 and Fe–balance. Potable water was used for casting the concrete specimens.

Determination of migration efficiency of MCI

Concrete specimen preparation

Concrete disks of size 85 mm in diameter having a thickness of 25 mm or 40 mm were cast and cured in water for 14 days. Cubical concrete specimens of 100 mm in size were cast along with the concrete disks for determining the compressive strength at the end of 14 days. After 14 days, the compressive strength was determined as per BIS 516-1974.[25]

Steel specimen preparation

From 16 mm diameter deformed bar, 1×1 cm square steel specimen was cut and brazed with 3 mm (dia.) $\times$ 15 cm length copper rod. Then this assembly was encapsulated in epoxy resin leaving an exposed area of 1 cm^2. Initially the mill scale was removed by mechanical grinding and polishing with SiC paper starting from 3/0 down to 5/0. Finally the specimen was degreased with trichloroethylene.

Migrating corrosion inhibitor

Migrating corrosion inhibitor is a liquid admixture consisting of N-N-dimethyleethanolamine (inhibitor) and alcohol (carrier) dissolved in water. The inhibitor

(amine) having a chemical formulae of $C_4 H_{11}NO$. Two concentrations, namely 9 and 2·73% v/v were studied. These concentrations are equivalent to application rates of 2·45 kg m^{-3} and 0·5 kg m^{-2} respectively as recommended by the manufacturer: the former is generally recommended for the repair of corroded concrete structures where MCI is added along with repair mortar whereas the latter is used for spraying on newly built structures.

Studies in 0·04 N NaOH solution

I_{corr} was determined by kept immersing the steel specimen directly in 0·04 N NaOH solution containing 9 and 2·73% v/v concentration of MCI. The experiment was conducted after 48 h of immersion in solution. The experiment was also conducted in presence of 1000 ppm of chloride.

Diffusion test

The migration efficiency of the inhibitor through the concrete was studied using the diffusion test cell shown in Fig. 1. The concrete disk was fixed between two cylindrical polyvinyl chloride (PVC) containers. The right side of the cell was filled with 0·04 N NaOH solution containing a known amount of inhibitor whereas the left side of the compartment was filled with only 0·04 N NaOH solution. The steel specimen was kept immersed in the solution on the left side of the cell. Before conducting the polarisation experiment, potential measurements were carried out periodically using a high input impedance multimeter. Potentiodynamic polarisation was performed using a three electrodes arrangement consisting of a steel specimen as a working electrode, titanium substrate insoluble anode as a counter electrode and saturated calomel electrode as a reference

Table 2 Composition of cement

	Weight, %
Oxides	OPC
SiO_2	20–21
Al_2O_3	5·2–5·6
Fe_2O_3	4·4–4·8
CaO	62–63
MgO	0·5–0·7

Table 3 Grading of coarse and fine aggregate

Coarse aggregate		Fine aggregate	
Sieve size, mm	Cumulative percentage retained, %	Sieve size, mm	Cumulative percentage retained, %
16	44·07	4·75	0
12·5	76·38	0·600	49
10	91·99	0·300	85
4·75	100	0·150	97
		<0·150	100

Table 1 Details of concrete mix proportions

Grade	W/C ratio	Cement, kg m^{-3}	Water, kg m^{-3}	Fine aggregate, kg m^{-3}	Coarse aggregate, kg m^{-3}	Slump, mm	Compressive strength at 14 days, MPa
M20	0·67	284	190	770	1026	50	29
M30	0·54	352	190	739	1026	30	39
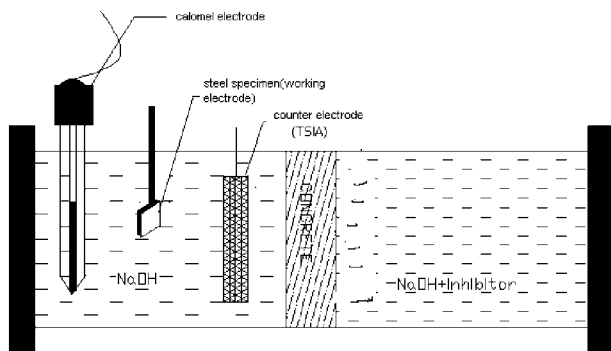
1 Schematic diagram of diffusion test cell

2 Rebar arrangement in 100 size cubical concrete specimen

electrode. Using the potentiostat Solartron model no. 1285, the potentiodynamic polarisation study was conducted by shifting the potential by ± 200 mV from the open circuit potential at a scan rate of 1 mV s^{-1}. The experiment was performed periodically at different intervals of time, namely 0, 2, 3, 7, 10, 15 and 18 days. The migration efficiency of the inhibitor was studied through 25 and 40 mm thickness of low density (20 MPa) and moderate density (30 MPa) concretes. Experiment was conducted on duplicate specimens and the average value has been reported.

From the E–log i plot, I_{corr} was determined using the software 'Corrware'. The results were compared with the control in which both side of the diffusion cell was filled with only 0·04 N NaOH solution. The reduction in corrosion current from the initial value indicates the migration of inhibitor through the concrete. By comparing the initial value of I_{corr} with I_{corr} at the end of test period, namely 2 and 15 days, the migration efficiency was calculated as

$$\text{Migration effiiciency} = \frac{I_{corr,i} - I_{corr,f}}{I_{corr,i}} \times 100 \qquad (1)$$

where $I_{corr,i}$ is initial corrosion current density and $I_{corr,f}$ is final corrosion current density at the end of the test period.

Determination of diffusion coefficient of MCI

From the migration efficiency of MCI, the quantity of inhibitor C_x was calculated from the initial concentration C_s. According to Fick'second law of diffusion, the diffusion coefficient of MCI was calculated using the following equation

$$C_x = C_s \left\{ 1 - erf \left[\frac{x}{2 \left(D_{app} t \right)^{1/2}} \right] \right\} \qquad (2)$$

where C_x is MCI concentration at known depth, C_s is initial concentration (mol cm^{-3}), x is cover in concrete (cm), D_{app} is apparent diffusion coefficient of MCI (cm^{-2} s) and t is period (s).

After determining the C_x at 25 and 40 mm thickness, the concentration versus thickness was plotted. By fitting this curve in equation (2), the diffusion coefficient of MCI was calculated.

Protection efficiency of inhibitor in chloride admixed concrete

Concrete specimen preparation

Cubical concrete specimens of 100 mm in size were used for determining the protection efficiency of inhibitor in
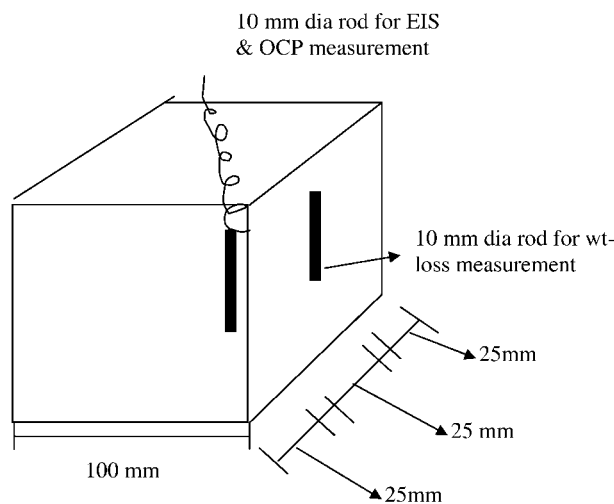
presence of chlorides as shown in Fig 2. A rod of 10 mm in diameter and 70 mm long was taken and its top and bottom were sealed using epoxy resin by leaving an exposed length of 5 cm. From this rod, electrical leads were taken and sealed. Then it was embedded at a cover of 25 mm from one side of the specimen. For determining the corrosion rate from weight loss measurements, another rod of similar dimension was also embedded as shown in Fig 2. Before embedding, the initial weight of the rod was noted. In one set of specimens, 1%NaCl by weight of cement was added at the time of casting and in another set of specimen no chloride was added to the concrete. Duplicate specimens were cast. After demoulding, the concrete specimens were cured for 14 days. After that, the specimens were air cured for six days in indoor environment.

Method of application of inhibitor

Initially before the application of an inhibitor, the open circuit potential and polarisation resistance R_p of the rebar (using impedance technique) was measured. This initial value is treated as control, i.e. without presence of inhibitor. Then the inhibitor was sprayed on one side of the specimen using a spray gun. The spraying was done for four times and the drying time allowed between two successive spraying was 6 h. The total amount of MCI applied on the concrete surface was 0·5 kg m^{-2}.

Method of measurement

In MCI treated concrete, the open circuit potential of the rebar was measured periodically using a high input impedance multimeter. The R_p value of the rebar was determined using impedance technique. Eletrochemical impedance measurements were made on MCI treated concrete specimens using three electrode arrangements. Stainless steel of 13 cm length in which saturated calomel electrode was centrally embedded in PVC sheet as described in Ref. 26 was used. While making measurements, a wetted sponge was inserted between the assembly and the concrete surface. Chloride solution was used as the wetting solution so as to reduce the contact resistance between the electrode assembly and the concrete. Rebar embedded in the concrete acted as the working electrode. Using electrochemical impedance analyser model no. 6310, the frequency between 100 kHz and 10 mHz was applied with an ac amplitude
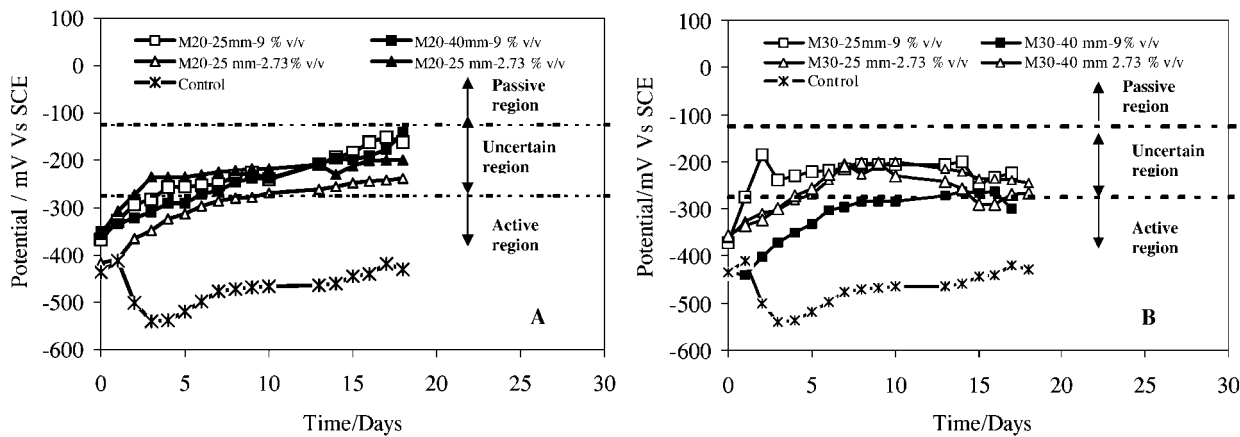
a 20 MPa concrete; *b* 30 MPa concrete

3 Potential time behaviour of steel versus migration of MCI under diffusion test

of 20 mV. The measurements were made periodically. The impedance values were plotted on the Nyquist plot. From the Nyquist plot, using the software 'Z view', the concrete resistance R_c and polarisation resistance R_p were determined by extrapolating the high frequency arc (100 kHz–10 Hz) and low frequency arc (100 Hz– 10 mHz) respectively. From the Bode plot, the phase angle of the rebar at maximum frequency was compared in 0 and 1%NaCl added concrete.

Exposure conditions

Migrating corrosion inhibitor treated concrete specimens were initially exposed to bare outside environment for a period of 70 days. During this period, potential and R_p were measured periodically. Then salt solution was sprayed on 0%NaCl added concrete specimens while potable water was sprayed on 1%NaCl added concrete specimens to initiate the corrosion of rebar. The specimens were exposed under this condition for 450 days.

Corrosion rate from weight loss measurements

After 450 days of exposure, the specimens were broken and the rods were visually examined for the extent of rust .Then they were pickled in inhibited hydrochloric acid as specified in ASTM G1 (Ref. 27) and the final weights were measured. From the change in weight, the corrosion rate in mmpy was calculated as

$$\text{corrosion rate(mmpy)} = \frac{87 \cdot 6w}{DA\,T} \qquad (3)$$

where w is loss in weight (mgms), D is density of iron (gm cm^{-2}), A is area (cm^2) and T is time (h). By comparing the corrosion rate of rebar embedded in 1%NaCl added concrete with 0%NaCl added concrete, the inhibitor efficiency was calculated.

Results

Potential measurements in diffusion test cell

As per ASTM C 876,[28] the following criteria have been applied while interpreting the data

Potential versus SCE, mV	Probability of corrosion, %
More –ve than −275	.>90 (active)
Between −275 to −125	Uncertain
More +ve than −125	<10 (passive)

Concrete of 20 MPa

The potential time behaviour is shown in Fig 3*a*. It can be seen that in the case of control, the potential initially tends to move faster in the more negative direction and then it slowly moves in the more positive direction. However, at the end of 18 days, the potential remains in the highly active region.

On the other hand, in the presence of MCI, the potential tends to move in the more positive direction and soon reaches the uncertain region (either active or passive). It further moves in the positive direction. However, at the end of 18 days all the potential values are still in the uncertain region only. Obviously when the MCI concentration is as high as 9%, most positive value has been registered. Thickness variation has no significant effect.

Concrete of 30 MPa

The potential time behaviour is shown in Fig. 3*b*. The trend is almost similar to 20 MPa concrete. However, the shift in potential is quite small.

Comparing the potential value at the end of 18 days with the initial value, a potential shift of 150 mV is observed in 20 MPa concrete through 25 and 40 mm thickness of concrete. In the case of 30 MPa concrete, from the initial value a potential shift of 135 and 92 mV in 9 and 2·73% v/v concentration is observed. The potential shift is more in 9% v/v concentration than in 2·73% concentration.

I_{corr} versus time

In 0·04 N NaOH solution

I_{corr} values for steel immersed in 0·04 N NaOH solution with and without MCI are compared in Table 4. I_{corr} of steel in 0·04 N NaOH solution without MCI (control) is $21·51 \times 10^{-7}$ A cm^{-2} which is 61 times higher than in 0·04 N NaOH solution containing 9% concentration of MCI and 41 times higher at 2·73% v/v concentration. Comparing with the control, the inhibitor efficiency is >98%. The inhibitor ions present in the solution are able to react with the steel surface spontaneously and cause strong reduction in anodic reaction that reduces the I_{corr} tremendously.

The steel shows a highest I_{corr} value of $186·2 \times 10^{-7}$ A cm^{-2} in presence of 1000 ppm of chloride in 0·04 N NaOH solution. But at 2·73% v/v concentration of MCI with 1000 ppm of chloride, the

I_{corr} value is $4 \cdot 12 \times 10^{-7}$ A cm^{-2} which is 45 times less than that of 0·04 N NaOH solution without MCI. The inhibitor efficiency at 1000 ppm of chloride works out to be 98%. The results clearly indicated that the inhibitor is able to perform efficiently even in presence of chloride in the alkaline medium.

In diffusion test cell

Figure 4*a* shows the *E*–log *i* plot of steel in 0·04 N NaOH with time. From the plot it can be seen that the I_{corr} increases with time. Initially the value is $5 \cdot 42 \times 10^{-7}$ A cm^{-2} and increases to $20 \cdot 44 \times 10^{-7}$ A cm^{-2} at the end of 15 days. Although it is an alkaline solution the chloride ions present in the concrete disk (even cement containing 0·1% of chloride) leached and gets dissolved in 0·04 N NaOH solution. This is confirmed by determining the chloride ions with silver nitrate method. Initially the chloride ion concentration is 120 ppm and this increases to 320 ppm at the end of 15 days. The Cl/OH$^-$ ratio is 0·075 and this increases to 0·20 at the end of 15 days. Presence of chloride ion increases the I_{corr} value of rebar in the alkaline solution.

Figure 4*b*–*e* shows the *E*–log *i* plot of steel in the presence of MCI at 9% v/v concentration through 25 and 40 mm thickness of 20 and 30 MPa concrete respectively. With days, the polarisation curve shifts in the anodic direction. When compared with the control, it is observed that the passive region is more in anodic direction in all the curves. From Fig. 4*b*, it can be seen that at 25 mm thickness of concrete, E_{corr} of steel is −368 mV initially and shifted in the anodic direction with days and reached to the value of −306 mV at the end of 15 days. When MCI diffuses through the 40 mm thickness of concrete (Fig. 4*c*), the initial E_{core} value of −397 mV gets increased to more +ve potential value of −213 mV at the end of 15 days. Similarly in 30 MPa concrete the shift in E_{corr} in the anodic direction is observed. It is evident that the reduction of anodic current and shift in E_{corr} potential in the anodic direction confirms that MCI acts as an anodic inhibitor.

The I_{corr} values of steel in the presence of 9% and 2·73% concentration are given in Tables 5 and 6 respectively. At 9% v/v concentration (Table 5), in 20 MPa concrete, the initial I_{corr} value of $5 \cdot 42 \times 10^{-7}$ A cm^{-2} decreases to a very low value of $0 \cdot 69 \times 10^{-7}$ A cm^{-2} through 25 thickness of concrete, i.e., the final I_{corr} is 7·8 times less than that of the initial value. Through 40 mm thickness of concrete, the I_{corr} value decreases to $1 \cdot 43 \times 10^{-7}$ A cm^{-2} which is four times less than that of the initial value. Obviously the rate of migration decreases with the increase in the thickness of concrete. Similarly in 30 MPa concrete, the decrease in I_{corr} is 4 and 3·16 times less than that of initial value through 25 and 40 mm thickness respectively. Jamil *et al.*[21] observed reduction in R_p value after diffusion of MCI through 10 mm mortar thickness. They have that after 100 h of spraying I_{corr} get reduced to $4 \cdot 3 \times 10^{-9}$ A cm^{-2} from the initial value of $8 \cdot 71 \times 10^{-8}$ A cm^{-2}.

From Table 6, it can be seen that at 2·73% v/v concentration in 20 MPa concrete not much reduction in I_{corr} is observed with days through 25 mm thickness of concrete. But through 40 mm thickness, I_{corr} at the end of 15 days is $1 \cdot 15 \times 10^{-7}$ A cm^{-2} which is one-third of that of the initial value. Whereas in the case of 30 MPa concrete, through 25 mm thickness, the I_{corr} value at the end of 15 days is $1 \cdot 57 \times 10^{-7}$ A cm^{-2} which is one-third of that of initial value. The trend is not changed through 40 mm thickness of concrete. In 30 MPa concrete at both 9 and 2·73% concentrations, after 18 days the I_{corr} value is around $1 \cdot 5 \times 10^{-7}$ A cm^{-2}. At both the concentrations, the I_{corr} decreases to an average value of $1 \cdot 5 \times 10^{-7}$ A cm^{-2} irrespective of the thickness and strength of concrete.

From the above results it can be inferred that 2·73% v/v concentration is sufficient for protection of steel.

Migration efficiency of MCI

Table 7 compares the migration efficiency of MCI at both the concentrations in 20 and 30 MPa concrete. In 20 MPa concrete the migration efficiency at 9% v/v concentration is 87% through 25 mm thickness of concrete and it is 77% through 40 mm thickness. At 2·73% v/v concentration, it is 68% through 25 mm thickness of concrete whereas it is 81% through 40 mm thickness.

In 30 MPa concrete, at 9% v/v concentration the migration efficiency is 70% through 25 mm thickness of concrete and it is 68% through 40 mm thickness. At 2·73% v/v concentration also the efficiency is 71%.

Diffusion coefficient of MCI

Table 8 compares the diffusion coefficient of MCI at the end of 15 days. In 20 MPa concrete at 9%MCI, the diffusion value is $7 \cdot 20 \times 10^{-5}$ cm^2 s^{-1} and at 2·73%, the value increased to $10 \cdot 62 \times 10^{-5}$ cm^2 s^{-1}. In 30 MPa concrete, at 9%, the value is $3 \cdot 62 \times 10^{-5}$ cm^2 s^{-1} and it increased to $4 \cdot 48 \times 10^{-5}$ cm^2 s^{-1} at 2·73% concentration. The rate of diffusion in 20 MPa concrete is two times higher than that in 30 MPa concrete.

Protection efficiency of MCI in NaCl added concrete

Potential measurements

Figure 5 compares the potential time behaviour of rebar embedded in MCI treated concrete over a period of 450 days. Before the application of MCI, in 20 MPa 0%Cl$^-$ added concrete, initial potential value is −262 mV and it is −318 mV in 1%Cl$^-$ added concrete. After the application of MCI, the potential tends to move in the positive direction and remains in the passive region up to a period of 275 days. However, at the end of 353 days, potential value is −125 mV in 0%Cl$^-$ added concrete and it is −236 mV in 1%Cl$^-$ added concrete.

Table 4 Comparison of I_{corr} after 48 h immersion

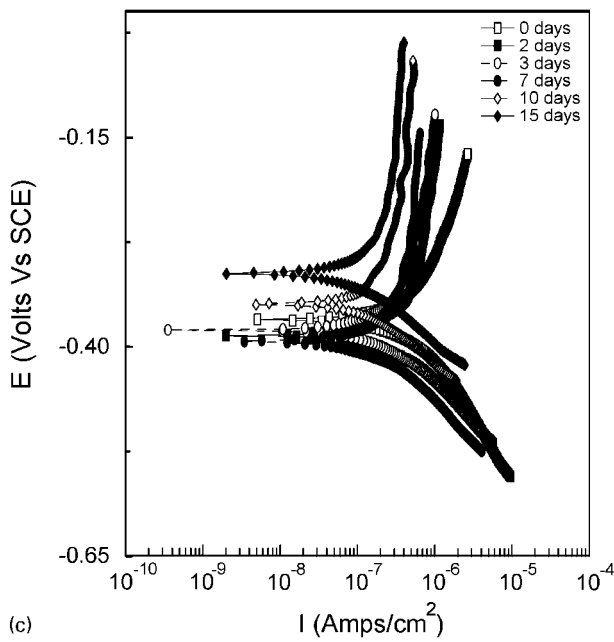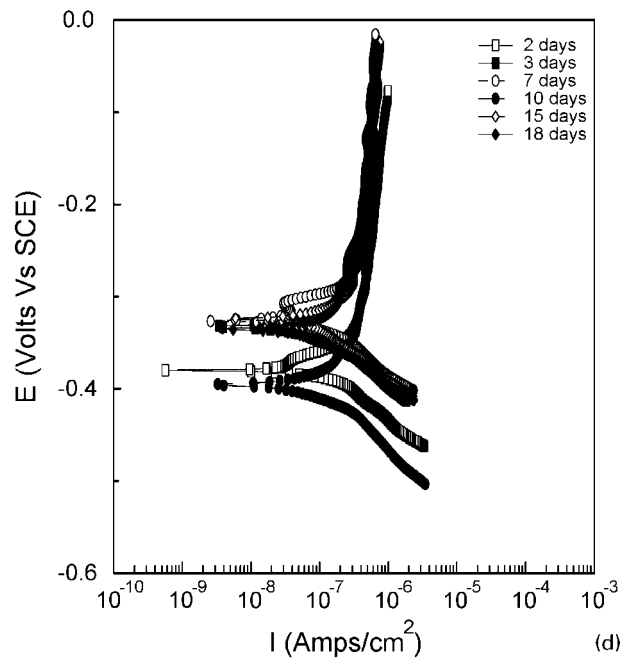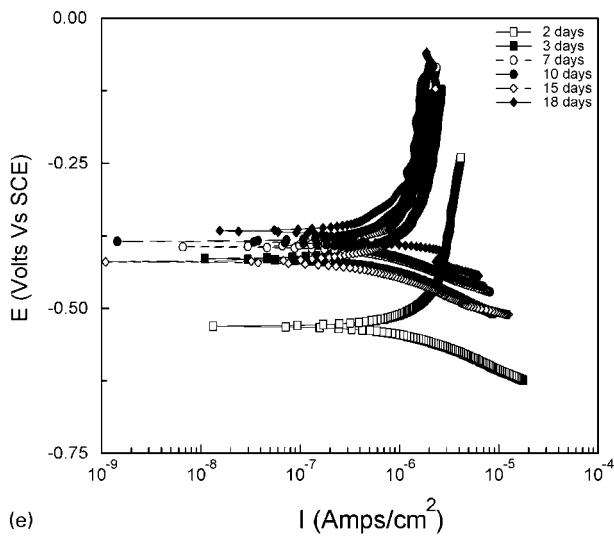| System	I_{corr}, A cm^{-2}	Inhibitor efficiency, %
0·04 N NaOH	$21 \cdot 51 \times 10^{-7}$	–
0·04 N NaOH + 2·73% v/v MCI	$0 \cdot 50 \times 10^{-7}$	98
0·04 N NaOH + 9% v/v MCI	$0 \cdot 35 \times 10^{-7}$	98
0·04 N NaOH + 1000 ppm Cl$^-$	$1 \cdot 86 \times 10^{-5}$	–
0·04 N NaOH + 2·73% v/v MCI + 1000 ppm Cl$^-$	$4 \cdot 12 \times 10^{-7}$	99
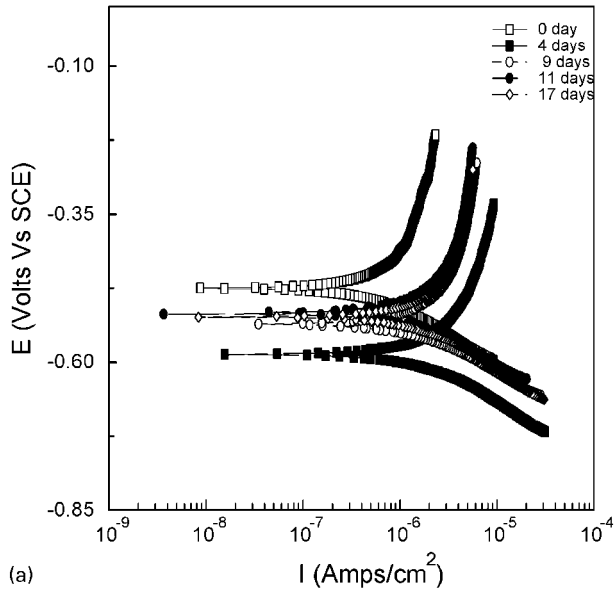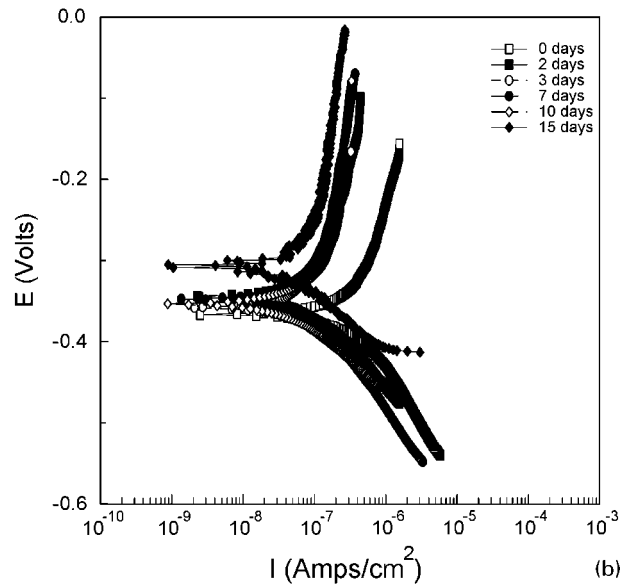
a control; *b* M20, 25 mm thick, 9% v/v; *c* M20, 40 mm thick, 9% v/v; *d* M30, 25 mm thick, 9% v/v; *e* M30, 40 mm thick, 9% v/v

4 Plots of *E* versus log *i*

Table 5 Comparison of I_{corr} under diffusion test cell (0·04 N NaOH+9% v/v of MCI)

	0·04 N NaOH+9% v/v MCI				Control	0·04 N NaOH+9% v/v MCI	
	20 MPa concrete		30 MPa concrete		20 MPa concrete	20 MPa concrete	
	Thickness, mm		Thickness, mm		Thickness, mm	Thickness, mm	
	25	40	25	40	25	25	40
Days	I_{corr}, $\times 10^{-7}$ A cm^{-2}		I_{corr}, $\times 10^{-7}$ A cm^{-2}		I_{corr}, $\times 10^{-7}$ A cm^{-2}	Percentage of variation, %	
0	5·42	5·70	5·42	5·70	5·42	±26	±1·86
2	1·20	3·22	2·18	3·09	–	±22	±18·71
3	1·12	2·74	2·12	1·85	21·51	±4	±4·98
7	0·75	2·43	1·59	2·31	18·55	±1·1	±4·08
10	0·67	1·43	1·93	1·54	16·51	±8	±21
15	0·69	1·32	1·64	1·47	20·44	±39	±21
18	–	–	1·36	1·80	–	–	–

Table 6 Comparison of I_{corr} under diffusion test cell (0·04 N NaOH+2·73% v/v MCI)

	0·04 N NaOH+2·73% v/v MCI				Control
	20 MPa concrete		30 MPa concrete		20 MPa concrete
	Thickness, mm		Thickness, mm		Thickness, mm
	25	40	25	40	25
Days	I_{corr}, $\times 10^{-7}$ A cm^{-2}		I_{corr}, $\times 10^{-7}$ A cm^{-2}		I_{corr}, $\times 10^{-7}$ A cm^{-2}
0	5·42	5·70	5·42	5·70	5·42
2	10·37	2·64	4·68	4·26	–
3	3·36	1·93	1·75	1·56	21·51
7	3·92	1·45	2·05	2·31	18·55
10	3·67	1·40	1·52	1·52	16·51
15	3·34	1·15	1·55	1·64	20·44
18	–	–	1·57	1·60	–

Table 7 Comparison of migration efficiency

	9% v/v concentration of MCI				2·73% v/v concentration of MCI			
	20 MPa concrete		30 MPa concrete		20 MPa concrete		30 MPa concrete	
	Migration efficiency, %		Migration efficiency, %		Migration efficiency, %		Migration efficiency, %	
	Thickness, mm		Thickness, mm		Thickness, mm		Thickness, mm	
Days	25	40	25	40	25	40	25	40
2	78	43	59	59	–	54	46	25
15	87	77	70	68	68	81	71	71

Table 8 Diffusion coefficient of MCI

Concrete grade	Concentration, % v/v	D_{MCI}, cm^2 s^{-1} (at the end of 15 days)
M20	9	$7·20 \times 10^{-5}$
M30	9	$3·62 \times 10^{-5}$
M20	2·73	$10·62 \times 10^{-5}$
M30	2·73	$4·48 \times 10^{-5}$
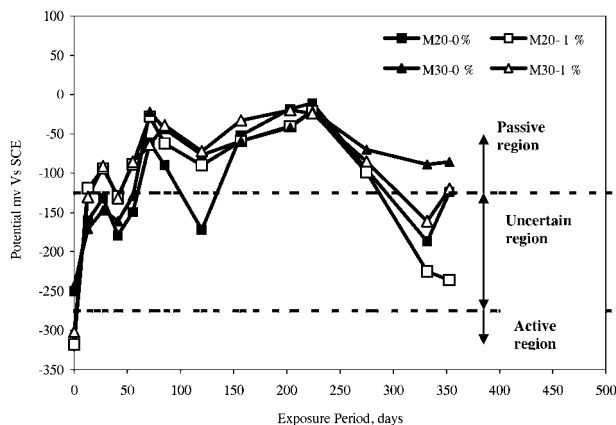
5 Potential time behaviour of rebar embedded in MCI treated concrete

As shown in Fig. 5, at both chloride levels the potentials are in the uncertain region.

In 30 MPa concrete, the potential of the rebar is in passive region throughout the exposure period. This is observed at both chloride levels. As cement content is higher in 30 MPa concrete it has higher chloride threshold value than 20 MPa concrete.[29] Combined effect of higher alkalinity and presence of inhibitor cause the stability of passive layer on the rebar throughout the exposure period. The potential value is well below −125 mV as specified in ASTM C876, this indicates that the rebar is in passive condition throughout the exposure period even in the presence of chloride.

R_p measurements

Figure 6 shows the assumed equivalent circuits at each stage of corrosion of rebar embedded in concrete. Figure 7a and b shows the Nyquist plot of rebar in 20 MPa concrete whereas Fig. 7c and d shows the Nyquist plot of rebar in 30 MPa concrete containing 0 and 1%NaCl respectively. The formation of passive layer by the adsorption of inhibitor, initiation of corrosion of rebar and uniform corrosion of rebar is clearly indicated by the Nyquist plot. It can be seen from Fig. 7 that at the end of 60 days, the slope of the low frequency arc varies from −1·5 to −2·89. As the slope is not exactly equal to −1, the warburg impedance (WI) behaviour is not observed. Because of the presence of large and non-ideal apparent interfacial capacitance at the steel/concrete interface, surface inhomogeneity on the rebar (ribbed bar) and heterogeneous nature of the concrete, the double layer capacitance of the rebar behaves like a constant phase element (CPE) rather than a pure capacitor.[30] In the equivalent circuit given in Fig. 6 CPE has been introduced (passive state). The formation of passive layer by the adsorption of inhibitor ions may also contribute to the

CPE behaviour of rebar. This is observed even in the presence of 1%NaCl added concrete (Fig. 7b and d). This indicates that the presence of MCI near the rebar displaces the chloride ions very effectively. At the end of 100 days, the slope of the low frequency arc in the Nyquist plot varies from −1·1 to 1·49 indicating the presence of WI due to initiation of corrosion. The reaction is now under diffusion control and according to the Nyquist plot obtained, the WI has been introduced in the equivalent circuit. At the end of 295 days in all most all the curves, the slope is less than in −1 and arc becomes much flatter and deformed indicating the progress of corrosion.

From Table 9, it can be seen that in 20 MPa concrete, the R_p value is 1629 Ω in 0%Cl⁻ added concrete. It is 548 Ω in 1%Cl⁻ added concrete which is one-third of that of 0%Cl⁻ added concrete. After application of MCI at the end of 60 days, it increases to 28 061 Ω. After exposure to chloride ions, R_p decreases to 7344 Ω at the end of 275 days. In 1%Cl⁻ added concrete R_p value increases to 50 551 Ω which is two times higher than that of 0%Cl⁻ added concrete. It indicates that the MCI effectively displaces the chloride ions and forms a passive layer. The passive layer is not stable in the presence of chloride and due to this R_p gets decreased to 3159 Ω at the end of 295 days.

Similarly in 30 MPa 0%Cl⁻ added concrete, the initial R_p value of 1444 Ω increases to 7875 Ω at the end of 295 days. In 1%Cl⁻ added concrete, the initial R_p value is 712 Ω which is half of that observed in 0%Cl⁻ added concrete. The highest R_p values of 37 124 and 59 583 Ω are observed in 0 and 1%Cl⁻ added concrete at the end of 60 days. After exposure to chloride, it gets decreased. But the value is still five to seven times higher than that of the initial value obtained in 0 and 1% chloride added concrete. Compared to 20 MPa concrete, R_p values are higher in 30 MPa concrete.

As shown in Fig. 8a at 60 days, the phase angle is >50° in all the concretes. Higher phase angle confirms the adsorption of inhibitors on the rebar.[31] The phase angle at the end of 295 days is 25°, 24° in 30 MPa, 0 and 1%NaCl added concrete (Fig. 8b) respectively which confirms disruption of passive layer by the chloride ions.

Corrosion rate from weight loss measurements

After 450 days of exposure, compared to 0%Cl⁻ added concrete, inhibitor efficiency (Table 10) decreases to 54% in 20 MPa 1%Cl⁻ added concrete. But in 30 MPa concrete no appreciable weight loss has been obtained in 0 and 1%NaCl added concrete.
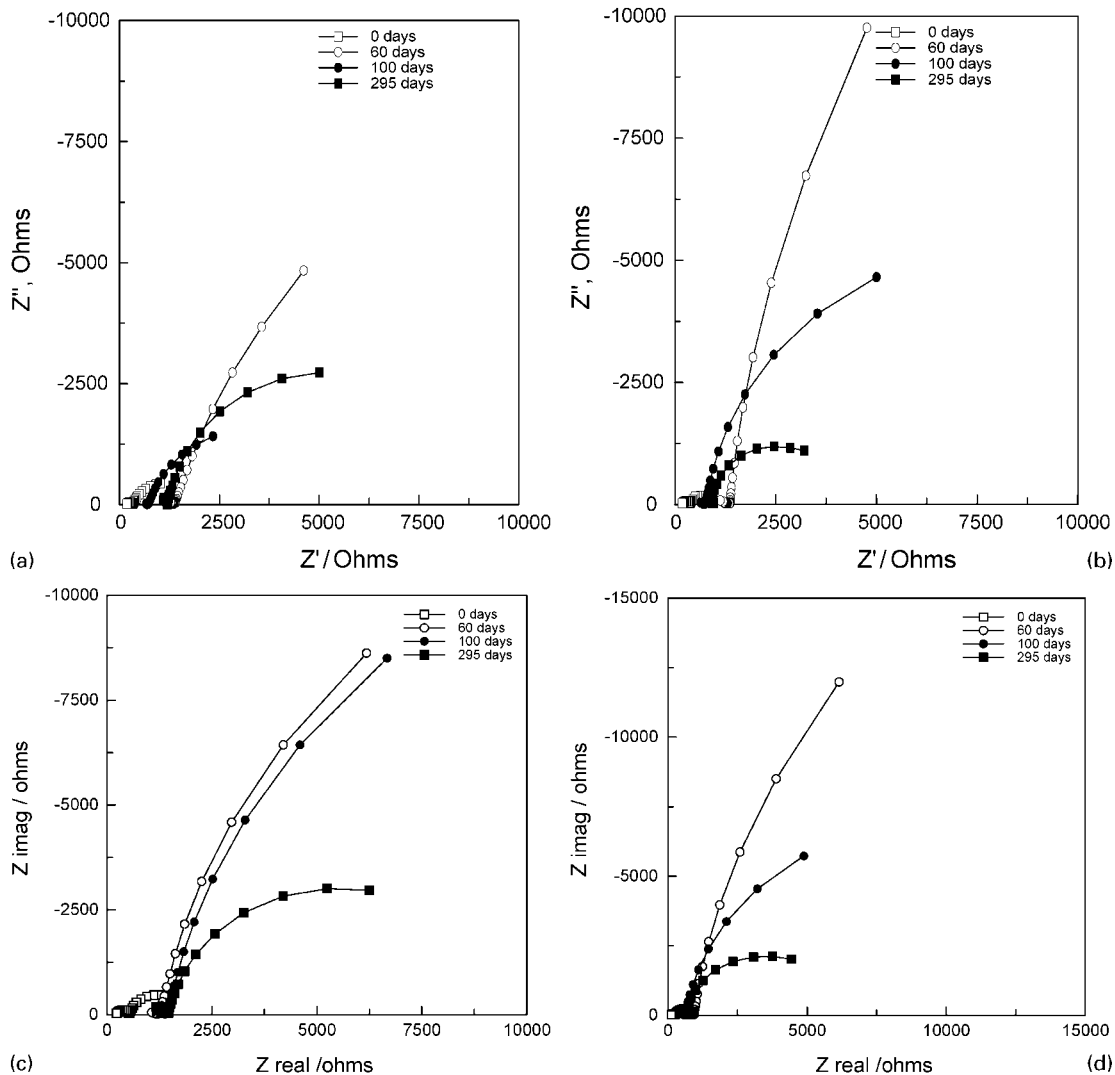
Discussion

The results obtained in this work clearly show that the inhibitor has the highest efficiency of 98% at the both
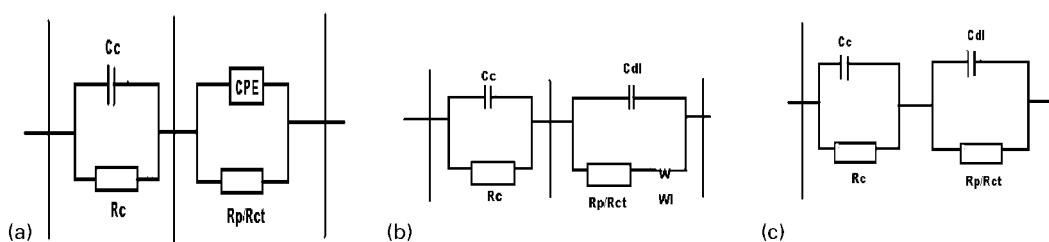
a passive state; *b* initiation of corrosion; *c* uniform corrosion

6 Assumed equivalent circuits

a M20, 0% chloride; *b* M20, 1% chloride; *c* M30, 0% chloride; *d* M30, 1% chloride
7 Nyquist plot of rebar embedded in concrete

concentrations in 0·04 N NaOH solution. Compared to control in the presence of 1000 ppm of chloride, the inhibitor efficiency is 99%. When the inhibitor migrates through the concrete its efficiency reduces to a minimum value of 70%. The efficiency is higher in low density concrete and at lower cover.

Protection mechanism

Table 11 summarises the E_{corr} and I_{corr} values of steel in the presence of 9 and 2·73% concentrations. Compared to the control, the MCI reduced the I_{corr} by 20 times in both 20 and 30 MPa concretes. The nitrogen of amine group present in the MCI is capable of forming into a coordinate bond with metals and adsorb on steel. The adsorption of cations increases the over potential of metal ionisation and slows down the corrosion process. This is confirmed by shift in potential of a minimum 62 mV in the anodic direction and reduction in an anodic current by half of that of initial value as shown in Table 11. This is also observed in 30 MPa concrete at higher thickness at the end of 15 days. This adsorption process is not instantaneous. It requires a defined time

Table 9 Comparison of R_p values: 20 MPa versus 30 MPa concrete

Days	Percentage of NaCl added, %	20 MPa concrete			30 MPa concrete		
		R_s, Ω	R_p, Ω	Phase angle θ, °	R_s, Ω	R_p, Ω	Phase angle θ, °
0	0	178	1629	23	314	1444	16
60		1376	28 061	46	1225	37 124	54
100		703	5055	31	1418	32 657	52
295		1172	7344	15	665	7875	25
0	1	217	548	11	158	712	12
60		1367	50 551	64	919	59 583	63
100		746	12 660	43	608	16 818	50
295		298	3159	19	169	5443	24
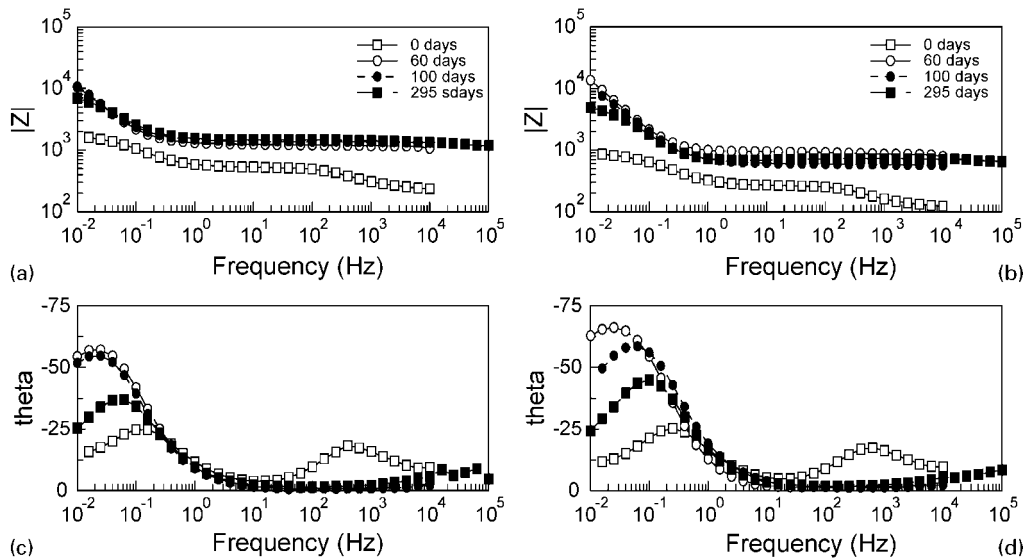
a M30, 0% chloride; *b* M30, 1% chloride
8 Bode plot of rebar embedded in concrete

period for the successful formation of the adsorbed layer on the target metal surface. It depends upon the surface area that the molecules occupy and molecular binding energy,[32,33] density and cover of concrete. Migrating corrosion inhibitor molecules are water soluble and possess higher binding energy to metal surfaces than the water dipoles. They create strong exothermic reactions, which can displace the surface water as well as chloride ions. A protective layer of hydroxide is formed on the steel exposed in alkaline medium (concrete and 0·04 N NaOH solution) having a pH value >12·5. This layer gets stabilised by adsorption of amines.[34] Nagayama and Kruger[35,36] suggest that the passive film is essentially composed of iron oxides. It may be either Fe_3O_4 or γ-Fe_2O_3. But Oranowska and

Szlarska-Smiolowska[37] showed that the passive films formed in alkaline solutions are closer to an iron oxihydroxides (FeOOH) than to Fe_2O_3 or Fe_3O_4.

Although initially the migration efficiency is less, after 10 days irrespective of the thickness and density of concrete a minimum of 70% migration efficiency is obtained at both the 9 and 2·73% v/v concentrations of inhibitor. In addition to molecule size and higher binding energy of inhibitor, the concentration of inhibitor also plays a role during the initial period of migration. As recommended by the manufacturer the 2·73% concentration is sufficient in the absence of chloride. Although this work did not envisage the determination of optimum inhibitor level, the results have clearly shown that spraying the concrete with

Table 10 Corrosion rate from weight loss measurements

| | Corrosion rate, mmpy | | | | Inhibitor efficiency |
| | 0%NaCl added | | 1%NaCl added | | |
Concrete	Average weight loss, gms	Average corrosion rate, mmpy	Average weight loss, gms	Average corrosion rate, mmpy	1%NaCl added
20 MPa	0·0128	0·0007	0·0248	0·0014	54
30 MPa	0·0000	0·0000	0·0078	0·0004	100

Table 11 Comparison of E_{corr} and I_{corr}: 20 MPa versus 30 MPa concrete

	9% v/v concentration of MCI							
	20 MPa concrete				30 MPa concrete			
	25 mm thickness		40 mm thickness		25 mm thickness		40 mm thickness	
Days	E_{corr}, mV	I_{corr}, A cm^{-2}	E_{corr}, mV	I_{corr}, A cm^{-2}	E_{corr}, mV	I_{corr}, A cm^{-2}	E_{corr}, mV	I_{corr}, A cm^{-2}
2 days	−368	1·20	−367	3·22	−430	2·18	−531	3·09
15 days	−306	0·69	−312	1·32	−301	1·64	−367	1·47
	2·73% v/v concentration of MCI							
2 days	−432	10·37	−398	2·64	−445	4·68	−423	4·26
15 days	−362	3·34	−319	1·1	−338	1·55	−345	1·64

2·73% v/v concentration can confer sufficient protection to the steel embedded in concrete.

When MCI is applied on concrete surface by spraying, some inhibitor ions may react with the hydrated cement products and some may get adsorbed on coarse aggregates. The amount of inhibitor ions adsorbed on the rebar surface is comparatively less than the inhibitor sprayed on the concrete. As indicated by higher R_p value and phase angle, passive layer has been formed even in presence of 1%NaCl added concrete. Similar results have been reported in concrete pore solution containing 4% v/v MCI.[14] After 60 days, when concretes were exposed to chloride environment, breakdown of passive film took place by chloride ions took place and this was indicated by a decrease in R_p value and phase angle at the end of 100 days. Thereafter the R_p value decreases continuously and attains a value in the range of 3159 – 7875 Ω depending upon the strength and amount of presence of chloride. The electrochemical impedance values suggest that the inhibitor molecules are probably displacing some hydrated layers of the surface film. Simultaneously this layer seems to have the capacity to bind chlorides through protonated aminogroups formed during initial displacement of the hydrated layers. In presence of chloride, the film formed becomes thicker, but more porous thus loosing its protective character.[38] This suggests that once the film breakdown occurs, it is incapable of reestablishing the passivity as the concentration of MCI near the rebar surface is low as it has not the capacity to complex with the chlorides.

From Table 9, it can be seen that the resistance of the concrete R_s at the end of 60 days increases to 1376 and 1225 Ω from the initial values of 178 and 314 Ω in 20, 30 MPa–0%NaCl added concrete. Similar trend is also observed in NaCl added concretes. R_s is 298 Ω in 20 MPa–1%NaCl added concrete end of 295 days and it is 169 Ω in 30 MPa–1%Cl⁻ added concrete. The presence and permeation of chloride decreases the R_s value with days. This value is higher in 0% chloride added concrete than in 1%NaCl added concrete. Although the resistance of the concrete does not directly indicate the passivation/ depassivation behaviour of rebar, it indicates the permeation of chloride with time.

Jamil *et al.*[21] reported the diffusion of MCI is independent of mortar thickness. But the present studies reveal that increase in thickness and density of concrete decreases the migration of MCI. Lower density concrete (20 MPa concrete) provides an easier path for the diffusion of MCI. This is confirmed by the higher (two times) diffusion coefficient of MCI in 20 MPa concrete than in 30 MPa concrete.

At the end of 450 days of exposure, very negligible corrosion rate is observed. But under field exposure conditions more chloride ions are expected to react the rebar surface with time. Under such conditions admixture of MCI during concreting may prove to be more effective than spraying on concrete surface. The 'washing away' of MCI during exposure is very negligible as the amines have more affinity towards the steel surface and react spontaneously. When added with repair mortar/concrete its efficiency is increased because of instantaneous formation of passive layer and adsorption of more number of inhibitor ions on the rebar surface. When MCI is applied on the concrete surface, a minimum of 70– 100 days is required for the formation of passive layer.

Passive layer formation is not stable if the chloride concentration is >1%NaCl by weight of cement. In 30 MPa concrete it has performed better because of higher chloride threshold value of concrete. In high chloride environment, this inhibitor can be added along with the concrete at a minimum rate of 2·45 kg m⁻³.

Conclusions

1. Migration efficiency depends upon the initial surface concentration of inhibitor. It is more in 9% v/v than in 2·73% v/v concentration. Efficiency is around 80% for 20 MPa concrete and around 70% for 30 MPa concrete.

2. The rate of diffusion of MCI through 20 MPa concrete is two times higher compared to the rate through 30 MPa concrete.

3. Migrating corrosion inhibitor when used as an admixture at the time of casting may prove to be more effective than spraying on hardened concrete surface.

4. When MCI is sprayed on concrete surface, a minimum of 70–100 days will be required for the formation of stable passive layer on the rebar embedded in concrete. A minimum concentration of 2·45 kg m⁻³ is necessary for efficient protection.

5. As indicated by the R_p value, the passive layer formed by MCI is not stable in the presence of 1%NaCl in 20 MPa concrete because of its ineffectiveness in increasing the chloride threshold value. Because of higher chloride threshold value, MCI has performed better in 30 MPa concrete.

6. Potentiodynamic polarisation studies have shown that amino alcohol based MCI acts as an anodic inhibitor.

References

1. C. M. Hansoon, L. Mammmoliti and B. B. Hope: *Cement Concrete Res.*, 1998, **28**, (12), 1775–1781.
2. N. S. Berke: *Concr. Int.*, 1991, **13**, 24–31.
3. C. Andrade, C. Alonso, M. Acha and B. Malric: *Cement Concrete Res.*, 1992, **22**, 869–877.
4. S. A. Civjan, J. M. Lafave, J. Trybulski, D. Lovett, J. Lima and D. W. Pfeifer: *Cement Concrete Comp.*, 2005, **27**, 688–696
5. S. M. Trepanier, B. B. Hope and C. M. Hanson: *Cement Concrete Res.*, 2001, **31**, 713–720.
6. M.Duprat and F. Dabosi: *Corrosion*, 1981, **37**, 89–98.
7. D. Bjegovic, B. A. Miksic and R. D. Stehly: *Mater. Corros.*, 2000, **51**, 444–453.
8. B. Bavarian and L. Reiner: *Mater. Corros.*, 2001, **52**, 385–396.
9. D. Bjegovic, I. Stipanovic, M. Skazlic, K. Feric and I. Barbalic: Proc. European Corrosion Congress, Budapest, Hungary, September 2003, European Federation of Corrosion, Paper 219.
10. D. Bjegovic and B. Miskic: *Mater. Perform.*, 1999, **38**, (11), 52–60.
11. H. Saricimen, M. Mohammed, A. Quddus, M. Shameem and M. S. Barry: *Cement Concrete Res.*, 2002, **24**, 89–96.
12. G. Batis, A. Routoulas and E. Rakanta: *Cement Concrete Comp.*, 2003, **25**, (1), 109–112.
13. H. E. Jamil, A. Shriri, R. Boulif, C. Bastos, M. F. Montemor and M. G. S. Ferreira: *Electro. Chem. Acta*, 2004, **49**, 2753–2763.
14. H. E. Jamil, M. F. Montemor, R. Boulif, C. Bastos, A. Shriri and M. G. S. Ferreira: *Electro. Chem. Acta*, 2003, **48**, 3509–3518.
15. C. Alonso, C. Andrade, C. Argiz and B. Malric: *Cement Concrete Res.*, 1996, **26**, (3), 405–413.
16. U. Maedar: in 'Corrosion and corrosion protection of steel in concrete', (ed. R. N. Swamy), Vol. 2, 851–864; 1994, Sheffield, Sheffield Academic Press.
17. D. Bjegovic, L. Sipos, V. Ukrainczyk and B. Miksic: in 'Corrosion and corrosion protection of steel in concrete', (ed. R. N. Swamy), Vol. 2, 856–863; 1994, Sheffield, Sheffield Academic Press.
18. B. Elsener, M. Buchler, F. Stalder and H. Bohni: *Corrosion*, 2000, **56**, 727–734.

19. N. Blank, J. Goschnick, M. Grunze and U. Mader: Proc. Int. Conf. on 'Adhesion', Yokohama, Japan, November 1994, Faculdade de Engerharia.
20. A. D. Portanguen, W. Prince, T. Lutz and G. Arliguic: *Cement Concrete Comp.*, 2006, **27**, 679–686.
21. H. E. Jamil, A. Shriri, R. Boulif, C. Bastos, M. F. Montemor and M. G. S. Ferreira: *Cement Concrete Comp.*, 2005, **27**, 671–680.
22. W. Morris and M. Vazquez: *Cement Concrete Res.*, 2002, **32**, 259–267.
23. 'Specification for 43 grade ordinary Portland cement', IS 8112, BIS, New Delhi, India, 1989.
24. 'Specification for high strength deformed steel bars and wires for concrete reinforcement', IS 1786, BIS, New Delhi, India, 1985.
25. 'Method of test for strength of concrete', IS 516, BIS, New Delhi, India, 1959.
26. S. Sathyanarayanan, N. Panjali, K. Saravanan, S. Srinivasan and G. Venkatachari: *Cement Concrete Comp.*, 2006.
27. 'Standard practice for preparing, cleaning and evaluating corrosion test specimens', G1–90, ASTM, Philadelphia, PA, USA, 2000.
28. 'Standard test method for half-cell potentials of uncoated reinforcing steel in concrete', C876–91, ASTM, Philadelphia, PA, USA, 2001, Vol. 04.04, 42.
29. G. K. Glass and N. R. Buenfeld: *Corros. Sci.*, 1997, **39**, (5), 1001–1010.
30. A. Sagues, S. C. Kranc and E. I. Moreno: *Corros. Sci.*, 1995, **37**, (7), 1097–1113.
31. P. Gu, S. Alliott, R. Hristova, J. J. Beaudoin, R. Brousseau and B. Baldock: *ACI Mater. J.*, 1997, **94**, (5), 385–396.
32. B. A. Miksic, M. Travin and G. R. Sparrow: NACE Conf., April 1998, New Orleans, LA, USA, Paper No. 308.
33. R. E. Penn and J. A. Birkeameier: *J. Mol. Spectrosc.*, 1976, **62**, 4–16.
34. M. Duprat, N. Bui and F. Dabosi: *Corrosion*, 1979, 35, **9**, 392–403.
35. A. Nagayama and M. Cohen: *J. Electrochem. Soc.*, 1963, **110**, 67–680.
36. J. Kruger and J. P. Calvert: *J. Electrochem. Soc.*, 1967, **114**, 403–410.
37. H. Oranowska and Z. Szlarska-Smiolowska: *Corros. Sci.*, 1981, **21**, 735–742.
38. M. F. Motemor, A. M. P. Simoes and M. G. S. Ferreira: *Corrosion*, 1998, **54**, 347–354.